HHS Public Access

Author manuscript

Oncogene. Author manuscript; available in PMC 2016 April 07.

Published in final edited form as:

Oncogene. 2016 April 7; 35(14): 1750–1759. doi:10.1038/onc.2015.239.

Hyperactivated FRS2α-mediated signaling in prostate cancer cells promotes tumor angiogenesis and predicts poor clinical outcome of patients

Junchen Liu[a,*], **Pan You**[a,b,*], **Guo Chen**[a,c,*], **Xin Fu**[a,c], **Xiangfeng Zeng**[a,d], **Cong Wang**[a,e], **Yanqing Huang**[a], **Lei An**[a], **Xinhai Wan**[f], **Nora Navone**[f], **Chin-Lee Wu**[g], **Wallace L. McKeehan**[a], **Zhongying Zhang**[b], **Weide Zhong**[c], and **Fen Wang**[a]

[a]Center for Cancer and Stem Cell Biology, Institute of Biosciences and Technology and College of Medicine, Texas A&M Health Science Center

[b]Xiamen University Affiliated Zhongshan Hospital

[c]Department of Urology, Guangdong Key Laboratory of Clinical Molecular Medicine and Diagnostics, Guangzhou First People's Hospital, Guangzhou Medical University

[d]Institute for Tissue Transplantation and Immunology, Jinan University

[e]College of Pharmacy, Wenzhou Medical University

[f]The University of Texas MD Anderson Cancer Center

[g]Departments of Pathology and Urology, Massachusetts General Hospital and Harvard Medical School

Abstract

Metastasis of tumors requires angiogenesis, which is comprised of multiple biological processes that are regulated by angiogenic factors. The fibroblast growth factor (FGF) is a potent angiogenic factor and aberrant FGF signaling is a common property of tumors. Yet, how the aberration in cancer cells contributes to angiogenesis in the tumor is not well understood. Most studies of its angiogenic signaling mechanisms have been in endothelial cells. FRS2α is an FGF receptor (FGFR)-associated protein required for activation of downstream signaling molecules that include those in the MAP and AKT kinase pathways. Herein we demonstrated that overactivation and hyperactivity of FRS2α, as well as overexpression of cJUN and HIF1α, were positively correlated with vessel density and progression of human prostate cancer (PCa) toward malignancy. We also demonstrate that FGF upregulated production of vascular endothelial growth factor A (VEGF-A) mainly through increasing expression of cJUN and HIF1α. This then promoted recruitment of endothelial cells and vessel formation for the tumor. Tumor angiogenesis in mouse PCa tissues was compromised by tissue specific ablation of *Frs2α* in prostate epithelial cells. Depletion of Frs2α expression in human PCa cells and in a preclinical xenograft model, MDA PCa 118b, also significantly suppressed tumor angiogenesis accompanied with decreased tumor growth in the

Corresponding should be addressed to: Fen Wang, fwang@ibt.tamhsc.edu, Weide Zhong, wdezhong@21cn.com; or Zhongying Zhang, zzy11603@163.com.

*Equal contribution

bone. The results underscore the angiogenic role of FRS2α-mediated signaling in tumor epithelial cells in angiogenesis. They provide a rationale for treating PCa with inhibitors of FGF signaling. They also demonstrate the potential of overexpressed FRS2α as a biomarker for PCa diagnosis, prognosis, and response to therapies.

Introduction

Tumor angiogenesis is required for tumor growth and progression by supplying nutrients and oxygen as well as removal of harmful metabolites and waste products. Without new blood vessels, tumors cannot normally expand beyond 1 mm^3 [18]. Microvessel density is considered a negative prognostic indicator for cancer [35]. Therefore, anti-angiogenesis is an alternative approach for cancer therapy rather than to a direct attack on tumor cells [11, 38]. However, anti-angiogenesis therapies are also accompanied by side effects and tumors eventually become resistant to the therapy. Detailed mechanistic studies are urgently needed to fully understand how tumors evade treatments and develop drug resistance. The fibroblast growth factor (FGF) was one of the first and remains a major angiogenic growth factor that have receive extensive scrutiny [3]. Most of the mechanistic studies on the role of FGFs in angiogenesis have been focused on signaling in endothelial cells. How aberrant FGF signaling in the cancer cells contributes to angiogenesis of the tumor is still not clear.

The FGF family consists of 18 receptor-binding polypeptides that control a broad spectrum of cellular processes. FGFs exert their regulatory activities by activating FGF receptor (FGFR) tyrosine kinases encoded by four genes [19]. Both FGF and FGFR are expressed in a spatiotemporal- and cell type-specific pattern. They control embryonic development and maintains adult tissue homeostasis and function. Abnormal FGF signaling is often associated with cancer initiation and progression to malignancy [19]. FGFRs elicit signals through activating MAP kinase, phosphatidylinositol-3 kinase (PI3K), PLC-γ, and other pathways, either via FGF receptor substrate 2α (FRS2α) dependent or independent mechanisms. FRS2α is a broadly expressed membrane-bound adaptor protein that undergoes extensive tyrosine and serine/threonine phosphorylation upon FGFR activation. Disruption of *Frs2α* abrogates FGF-induced activation of MAP and PI3K [8, 10].

Prostate cancer (PCa) is the most commonly diagnosed cancer in American males. Extensive studies indicate that abnormal expression of the FGF or FGFR and aberrant activation of the FGF/FGFR signaling axis are associated with PCa development and progression. Amplification of the Fgfr1 gene frequently occurs in human PCa [25]. The acquisition of ectopic expression of FGFR1 in tumor epithelial cells where it is normally silent stands out as a remarkable change among FGFR isotypes [4, 7, 21, 33]. Forced expression of FGFR1 or multiple FGF ligands in prostate epithelial cells has been shown to induce prostate lesions in mouse models [1, 6, 14, 16, 20, 23, 24, 30, 32]. Ablation of *Fgfr1* or *Frs2α* significantly reduces development and progression of PCa induced by T antigens [37, 40]. FGF signaling promotes cell proliferation and reduces cell death. However, the full spectrum of how aberrant FGF signals contribute to PCa development and progression beyond driving high proliferative rate and low cell mortality of cancer epithelial cells is still not fully understood.

Herein we show that overexpression and elevated phosphorylation of FRS2α is associated with tumor angiogenesis as well as clinical features of human PCa. Ablation of *Frs2α* in prostate epithelial cells compromised angiogenesis in the TRAMP mouse prostate tumor model. Depleting FRS2α expression in human PCa cells also reduced their ability to recruit human umbilical cord endothelial cells (HUVEC) *in vitro* and host endothelial cells *in vivo*. A detailed analysis revealed that FRS2α-mediated signals in PCa cells contributed to tumor angiogenesis via promoting production of VEGF-A through HIF1α and cJUN pathways in the cells. This in turn recruited endothelial cells to the tumor. Thus, the results reveal a novel mechanism by which FRS2α-mediated signaling in PCa epithelial cells facilitates tumor angiogenesis within the microenvironment, unravel the potential of overexpressed FRS2α as a biomarker for PCa diagnosis, and provide a rationale for treating PCa based on inhibiting FRS2α-mediated signaling in epithelial cells or pro-angiogenic factors controlled by it.

Results

1. Overexpression of Frs2α in human PCa is associated with tumor angiogenesis and poor prognosis of PCa patients

FGFR1 is overexpressed in about 40% of human PCa [1, 21] and forced expression of ectopic FGFR1 in mouse prostate epithelial cells increases tumor angiogenesis [36]. FGF9 promotes VEGF-A expression in LNCaP cells [26]. However, whether aberrant FGF signaling and its key mediator for downstream signaling FRS2α is associated with and contributes to overall tumor angiogenesis in human PCa has not been established. We assessed the clinical relevance of FRS2α expression and its correlation with microvessel density in human PCa by immunohistochemistry with anti-FRS2α and immunostaining with anti-CD31 antibodies. Both analyses were carried out on the same slides from the MGH human prostate tissue microarrays (TMA) that comprised 225 PCa and 27 benign prostate samples (Fig. 1A). The samples were annotated with detailed patient follow up information, including PSA recurrence, Gleason Scores, pathological stages, patients' age, and survival time. Although only a small group of cases had very strong staining (scores 7–9), the majority of the PCa samples had a score between 4–6. This was higher than the expression score in the adjacent non-cancerous tissues (Fig. 1B). In addition, elevated expression of FRS2α was found in PCa with high Gleason scores and in patients with high serum PSA (Fig. 1C). To determine whether FRS2α expression correlated with the prognosis of PCa patients, the association of FRS2α expression and PCa metastasis, PSA recurrence time, and overall survival time of the 225 patients was analyzed (Fig. 1C). The data showed that the PSA recurrence-free survival and overall survival time of PCa patients were shorter in the groups exhibiting high FRS2α expression (score >3), compared to the group with low FRS2α expression (score≤3). Furthermore, appearance of metastases occurred faster in PCa exhibiting high FRS2α than those with low FRS2α expression. In addition, expression levels of FRS2α positively correlated with microvessel density determined by CD31 staining (Pearson correlation: $R=0.55$, $P<0.01$).

To further implicate activity of FRS2α in angiogenesis in human PCa tissues, levels of activity of FRS2α were assessed by immunochemical staining of activate FRS2α (phosphorylated) in a separa te PCa TMA. Expression of HIF1α, cJUN, and CD31 were also

assessed in the same array. This array included 99 primary PCa and 81 adjacent non-cancerous prostate tissue samples with the pathological features characterized by the vendor (Fig. 1D). The results showed that phosphorylation of FRS2α was higher in PCa than in benign tissues (2.23±1.78 vs 1.68±1.32, P<0.02) and that the expression of cJUN was higher in tumors with Gleason Score ≥7 than in those with Gleason Score ≤7. In addition, the level of activities of FRS2α measured by its phosphorylation positively correlated with expression of cJUN (r=0.358, p<0.001), but not with HIF1α (r=0.142, P=0.164), and CD31 (r=0.009, P=0.312).

We then further evaluated the correlation coefficients between Frs2α expression and cJun, Hif1a, and CD31 at the mRNA level in the Taylor dataset GSE10645 [25]. The results showed a positive correlation between Frs2α expression and cJun (r= 0.473, P<0.001), Hif1a (r=0.675, P<0.001), and CD31 (r=0.358, P<0.001) mRNA levels in the PCa tissues that comprise both epithelial and stromal cells. Since microvessel density correlates with poor PCa progression, the data further demonstrate that overexpressed FRS2α in the tumor promotes PCa angiogenesis and suggest that FRS2α affects the clinical course of human PCa, since microvessel density correlates with poor PCa progression. Together, the data also suggests that the level of FRS2α expression in PCa tissues can serve as a biomarker for predicting outcomes of PCa patients.

2. Ablation of *Frs2α* reduces angiogenesis in PCa

Ablation of *Frs2α* inhibits prostate tumor initiation, growth, and progression in the TRAMP mouse prostate tumor model [40]. To investigate whether ablation of *Frs2α* suppressed PCa angiogenesis in the model, *Frs2α* was ablated specifically in prostate epithelial cells by crossing the floxed *Frs2α* (*Frs2α*^{Flox}) mice with the ARR2Pbi-Cre transgenic mice (hereafter designated as *Frs2α*^{CN} for *Frs2α* conditional null). Prostate tumors were excised for examination from 5 month TRAMP mice. The *Frs2α*^{CN} tumors had less CD31^{+} endothelial cells than control *Frs2α*^{Flox} tumors. This suggests a reduction in vasculature of tumors deficient in *Frs2α*. To confirm this finding, immunostaining of the adjacent sections with additional microvasculature markers NG2 and lectin was carried out. Consistently, both NG2 and lectin stained cells in *Frs2α*^{CN} tumors were lower than those in *Frs2α*^{Flox} tumors. In addition, expression of CD31, NG2, and VE-cadherin mRNA levels were lower in *Frs2α*^{CN} tumors than those in control tumors (Fig. 2). Together, the results indicate that ablation of *Frs2α* results in reduced angiogenesis in the tumors.

3. Depletion of *FRS2α* expression in PCa cells compromises their ability to recruit endothelial cells via soluble factors

Since recruiting endothelial cells is a critical step in tumor angiogenesis, we then tested whether FRS2α was essential for PC3 human PCa cells to recruit endothelial cells via secretory factors. This was done by transfecting the cells with FRS2α specific siRNA to deplete FRS2α mRNA (Fig. 3A). The medium conditioned by the cells was collected and its activity for recruiting HUVECs was assessed by Transwell cell culture analyses (Fig. 3B). The results showed that relative to the control cells, PC3 cells with reduced FRS2α in the bottom chamber had a reduced ability to promote migration of HUVECs in the upper chamber. Moreover, the medium conditioned by FRS2α-depleted PC3 cells also had reduced

capacity to promote HUVEC cell migration in the scrape wound healing assay (Fig. 3C). The results indicate that FRS2α-mediated signals in PCa cells result in release of soluble factors that recruit endothelial cells. Endothelial cells can form luminal capillary-like structures in Matrigel *in vitro*. This characterizes an angiogenic switch that is stimulated by secretory factors from tumor cells [2, 5, 28]. We tested the activity of PC3 cell conditioned medium for promoting endothelial cell tube formation. Again, the medium conditioned by FRS2α-depleted PC3 cells was also less active in inducing tube formation of HUVECs compared with that of control PC3 cells (Fig. 3D). Notably media conditioned by these two lines of PC3 cells did not affect HUVEC proliferation (data not shown).

We then determined whether depletion of FRS2α expression in PCa cells also compromised their ability to induce endothelial migration and invasion *in vivo*. This was accomplished by depletion of FRS2α expression in PC3 cells by stable expression of FRS2α shRNA (Fig. 4A). The FRS2α-depleted PC3 cells were mixed with Matrigel, which were then implanted into the flanks of immune-deficient nude mice. The Matrigel plugs were harvested at day 14 after the implantation. The pale tone of the Matrigel plugs containing FRS2α-depleted PC3 cells relative to the red color of the plugs containing control PC3 cells indicated a reduced blood vessel density in the FRS2α-depleted group (Fig. 4B). Immunostaining with $CD31^+$ cells confirmed that endothelial cell content in the Matrigel plugs was reduced in the FRS2α depleted group (Fig. 4C). The results further indicate that FRS2α-mediated signals in PCa cells underlie recruitment of endothelial cells to tumors formed by PCa cells and thus angiogenesis of the tumors. Furthermore, quantitative RT-PCR analyses of the RNA extracted from the Matrigel plugs containing the tumors showed that depletion of FRS2α in PC3 cells reduced human VEGF-A expression from the PC3 cells along with endothelial cell specific RNAs from hose mouse. This further demonstrated that FRS2α-mediated signals in PCa cells promoted recruitment of host endothelial cells to the tumor (Fig. 4D).

4. Ablation of *Frs2α* in PCa cells reduces Vegf-A expression via down-regulation of Hif1a and cJun expression

Since VEGF-A is a key angiogenic factor, we then employed quantitative RT-PCR analyses to assess *Vegf-a* expression in TRAMP tumors bearing $Frs2\alpha^{Flox}$ or $Frs2\alpha^{CN}$ alleles. In comparison with $Frs2\alpha^{Flox}$ tumors, the expression of *Vegf-a* in $Frs2\alpha^{CN}$ tumors was reduced (Fig. 5A). To investigate the mechanism underlying regulation of *Vegf-a* by FRS2α-mediated signals, quantitative RT-PCR analyses were employed to assess the expression of potential *Vegf-a* upstream regulators. The expression of *Sp1*, *Hif1a*, *Ap2,* and *cJun* was reduced in $Frs2\alpha^{CN}$ tumors at the mRNA level. Furthermore, immunostaining showed that expression of HIF1α and cJUN was downregulated at the protein level in $Frs2\alpha^{CN}$ prostate and PCa (Fig. 5B). There were no changes in SP1 and AP2 expression in the $Frs2\alpha^{CN}$ prostate (data not shown), possibly due to other redundant upstream regulators. Western analyses further confirmed that expression of cJUN and HIF1α were reduced at the protein level (Fig. 5C). The results suggest that downregulation of these two upstream regulators contribute to reduced expression of *Vegf-a* in $Frs2\alpha^{CN}$ prostate and prostate tumors.

We also noted that depletion of FRS2α also compromised Vegf-a, cJun, and Hif1a expression in human PC3 cells although the expression of Sp1 and Ap2 was not affected

(Fig. 6A). We then focused our efforts to determine whether cJUN and HIF1α were required for *Vegf-a* expression in human PCa cells. A luciferase reporter construct driven by the *Vegf-a* promoter was used to determine whether depletion of the two transcription factors compromised expression of the reporter. Consistently, the results showed that depletion of cJUN and HIF1α, but not SP1 or AP2, in PC3 cells reduced expression of the luciferase reporter, suggesting that SP1 and AP2 were dispensable for Vegf-a expression in PC3 cells (Fig. 6B). To further determine whether cJUN, HIF1α, SP1, and AP2 mediated FRS2α signals were required to support Vegf-a expression in PC3 cells, expression of these transcription factors was depleted with siRNA. Western blot analyses showed that expression of VEGF-A was reduced in the cells treated with cJun and Hif1a siRNA (Fig. 6C). Consistently, overexpression of both HIF1α and cJUN in FRS2α-depleted PC3 cells partially restored their activity in promoting HUVEC migration (Fig. 6D). Furthermore, ChIP assays revealed that capture of the *Vegf-a* promoter region by cJUN in pull-fown assays was reduced in PC3 cells depleted of FRS2α (Fig. 6E, panels a&b). Since HIF1α is unstable in the normoxic condition and thus it is difficult to do ChIP assays using cultured cells, similar ChIP experiments for HIF1α were carried out with $Frs2\alpha^{CN}$ and control PCa tissues (Fig. 6E, panels c&d). The Vegf-a promoter sequence pulled down by HIF1α was reduced in $Frs2\alpha^{CN}$ tumors compared to control tumors. The data demonstrate that HIF1α and cJUN are involved in upregulation of VEGF-A expression by FRS2α-mediated signals in PCa cells.

We then assessed the role of FRS2α in human PCa in bone that is the most common site of lethal PCa metastasis. The expression of FRS2α was depleted in tumor cells isolated from MDA PCa 118b tumors, a preclinical human PCa xenograft model, by infection with adenovirus carrying shFrs2α (online Fig. 1A). The cells were then implanted to the femurs of SCID mice for assessing their capacity for growth in bone [16]. FRS2α-depleted cells exhibited a lower tumor forming capacity in the mouse femurs than did control cells (online Fig. 1B&C). This suggests that the FRS2α deficiency reduces growth of the tumor cells in bone. Moreover, the density of $CD31^+$ endothelial cells was reduced in the FRS2α-depleted tumors (online Fig. 1D), indicating that the angiogenesis in the tumor was compromised by depletion of FRS2α.

Discussion

In this report, we demonstrated that hyperactivation of FRS2α-mediated angiogenic signaling was associated with tumor angiogenesis and poor clinical features of human PCa. This included high blood vessel density, high-Gleason Score, and high serum PSA. Furthermore, high FRS2α expression correlated with poor outcomes of PCa patients. These included high metastatic rates, shortened time to tumor recurrence, and shorter survival times. We also showed that FRS2α underlies the previously established ability of FGF to elicit angiogenic signals. Ablation of *Frs2α* in prostate epithelial cells reduced VEGF-A expression through downregulating cJUN and HIF1α expression. This was accompanied by inhibition of tumor angiogenesis and tumor growth in mouse PCa models. Depletion of FRS2α in human PCa cells also compromised the capability of the cells to recruit endothelial cells both *in vivo* and *in vitro*. Our results suggest that hyperactivation of the FRS2α-mediated angiogenic pathway can be used as biomarkers for PCa diagnosis and

prognosis and particularly efficacy of treatments. They also suggest that suppressing FRS2α-mediated angiogenic signaling is promising for development into a strategy for PCa treatment.

Fgfr1 is overexpressed in about 40% of human PCa [1, 21]. Amplification of Frs2α and activation of the FGFR/FRS2α signaling pathway has been shown in liposarcomas [34, 39]. It has been previously reported that although no significant differences in Frs2α and Frs2β expression in small samples of human PCa were detected. However, double depletion of FRS2α and FRS2β in human PCa cells reduces cell proliferation, migration, and invasion, as well as increase susceptibility to cytotoxic irradiation [29]. In this report, we report data derived from three sample pools that expression and activation of FRS2α were increased in human PCa at the protein level with the MGH PCa TMA, at the activity level with the commercial available PCa TMA, and at the mRNA level in the Taylor dataset. The consistent conclusion derived from both TMA and the online dataset indicates that neither ethnic factors nor detailed screening methods affected the conclusion that increased levels of FRS2α correlate with tumor angiogenesis in human PCa.

The levels of FRS2α phosphorylation in PCa, which indicated its activation, were higher than in adjacent non-cancerous tissues, although the statistical data showed that the difference was moderate. We found that the FRS2α phosphorylation levels in tissues adjacent to the tumor varied significantly. Some areas had a relatively high phosphorylated FRS2α although others had low to undetectable phosphorylated FRS2 α. It is possible that the phosphorylation of FRS2α in para-cancer tissues is affected by PCa adjacent to them. In resting adult mouse prostates, expression of FRS2α in luminal epithelial cells is below the detection limit of immunostaining [40]. Therefore, it is necessary to assess phosphorylated FRS2α in normal prostate tissues in order to determine whether phosphorylated FRS2α can be used as a biomarker for PCa diagnosis and prognosis. Nevertheless, the data here demonstrated that hyperactivation of FRS2α-mediated angiogenic signaling is associated not only with the malignance of prostate lesions, but also with poor prognosis for patients bearing PCa.

Furthermore, the results were consistent with the report that Fgfr1 is overexpressed in PCa and that overexpression of FGF9 increases VEGF-A expression in LNCaP cells and therefore predicts bone metastasis and poor prognosis of PCa [16, 26]. It has been shown that expression of ectopic FGFR1 in mouse prostate epithelial cells is oncogenic and that ectopic FGFR1 signaling promotes tumor angiogenesis [36]. In addition, expression of a constitutively active mutant of FGFR1 also increases *Vegf1* expression and angiogenesis in hepatocellular carcinoma [12]. However, whether FRS2α is required for the angiogenic signals elicited by FGFR1 have not been reported. Our results not only confirm the tumor angiogenic roles of ectopic FGF signaling, but also unravel its underlying mechanism. This shines new light on potential for development of new PCa treatments based on disruption of the FRS2α-mediated tumor angiogenic signaling axis.

Depletion of FRS2α in PCa cells reduced recruitment of endothelial cells to tumors via secreted factors. This suggests that FRS2α-mediated signals in tumor cells are involved in communication of tumor cells with host cells in the surrounding microenvironment. The

results are consistent with our recent report that human PCa cells induce host bone cells to overexpress FGF2 and FGFR1, suggesting that the FGF axis mediates a synergistic interaction between PCa cells and bone cells in the tumor microenvironment to support metastatic PCa growth in bone [31]. Since PCa cells overexpress FGFR1 that FGF2 is an activating ligand for FGFR1, the host cell FGF2 in turn will also enhances the angiogenic activity of PCa cells mediated by the FRS2α pathway. We further demonstrated here that depletion of FRS2α in MDA PCa 118b cells reduced tumorigenesis in the bone as well as reduced blood vessel density in the prostate tumors hosted by bone (online Fig. 1). The results further indicated the importance of FRS2α-mediated signals in the crosstalk between PCa and host cells in the bone microenvironment.

The Vegf-a promoter region contains multiple consensus transcriptional regulatory factor binding sites, which include SP1/SP3, AP1, AP2, Egr1, STAT3, and HIF1α [22, 27]. Although SP1 and AP2 can serve as downstream signaling molecules in the FGF pathway, overexpression of both AP2 and SP1 failed to restore the expression of VEGF-A in FRS2α-depleted PCa cells. This suggests that the two transcription factors are not sufficient to mediate angiogenic signals elicited by the FRS2α pathway. Moreover, ablation of *Frs2α* did not affect expression of the two transcription factors. The results suggest that regulators other than the FRS2α-pathway that are upstream of VEGF-A may control VEGF-A expression via these transcription factors. Future efforts are needed to identify the upstream regulators for SP1 and AP2 involved in control of VEGF-A expression.

In summary, we report here that FRS2α-mediated signals contribute to PCa angiogenesis. The depletion of FRS2α expression suppressed PCa tumor angiogenesis and tumor growth. Since FRS2α is a major mediator of the FGFR1 signaling complex at the intracellular membrane boundary, it likely accounts for the effects of hyperactive FGFR1 in tumors on tumor angiogenesis. Furthermore, hyperactivation of the FRS2α signaling pathway was associated with blood vessel density and pathological features of human PCa. The results suggest that suppression of the FRS2α-mediated pathway may be of therapeutic value for PCa therapies and that the hyperactive FRS2α signaling pathway is a potential biomarker for PCa diagnosis.

Materials and Methods

Animals and isolation of tissues

All animals were housed in the Program of Animal Resources of the Institute of Biosciences and Technology, Texas A&M Health Science Center, and were handled in accordance with the principles and procedures of the *Guide for the Care and Use of Laboratory Animals*. All experimental procedures were approved by the Institutional Animal Care and Use Committee. Mice carrying the *ARR2PBi-Cre* transgenic [15], *Frs2α*^{flox} [17] and TRAMP transgenic [9] alleles were maintained and genotyped as previously described. A total of 40 TRAMP mice were generated for this study. No randomization was used in this study.

Histological and immunostaining

Prostate or PCa tissues were fixed, dehydrated, embedded, and sectioned according to standard procedures [40]. Antigens were retrieved by boiling in the citrate buffer (10 mM) for 20 minutes or as suggested by manufacturers. All sections were incubated with primary antibodies diluted in PBS at 4°C overnight. The rabbit anti-cJUN (1:200) was purchased from Cell Signaling Technology (Beverly, MA); rabbit anti-HIF1α (1:200) and rabbit anti-CD31 (1:200) from Abcam (Cambridge, MA); mouse anti-CD31 (1:200) antibodies from Novus Biologicals (Littleton, CO); rabbit anti-FRS2α from Santa Cruz (Santa Cruz, CA); rabbit anti-NG2 antibodies from Chemicon (Billerica, MA); biotinylated-isolectin B4 from Vector Labs (Burlingame, CA). Specifically bound antibodies were detected with alkaline phosphatase staining or FITC-conjugated secondary antibodies (Life Technologies, Grand Island, NY).

For expression of Frs2α and CD31 in human PCa, the Massachusetts General Hospital (MGH) PCa TMA was used. It includes 240 consecutive patients with PCa who underwent radical prostatectomy at the MGH from September 1993 to March 1995 [41]. For analyses of phosphorylation of FRS2α in PCa, the human PCa TMA from the Shanghai Outdo Biotech Co, LTD (Shanghai, China, Cat No: HPro-Ade180PG-01) was used. It includes 99 primary PCa and 81 adjacent non-cancerous prostate tissues with the pathological features characterized by the vendor [13]. Two experienced pathologists independently scored the results without any information about the samples. Only epithelial staining was counted. The scores were compared, and discrepant scores were subjected to re-examining by both individuals to achieve a consensus score. Immunostaining of PCa and stromal cells were evaluated separately. The percentage of positive cells was calculated and categorized as following: 0, 0 %; 1, 1–10 %; 2, 11–50 %; 3, 50 –75%; and 4, 75–100%. The staining intensity was visually scored and defined as 0, negative; 1, weak; 2, moderate; and 3, strong. Final immunoreactivity scores (IRS) were calculated for each case by multiplying the percentage and the intensity score. The specificities of the antibodies were validated as shown in online Fig. 2.

Matrigel plug

Young adult (8-week-old) male nude mice were used for the Matrigel plug assay. Cells ($1X10^6$) were infected with control or shFrs2 lentivirus before being mixed with 0.5 ml Matrigel on ice. The Matrigel-cells mixtures were then implanted into the right flank of the mice. The plugs were harvested 14 days after the implantation.

Cell culture and conditioned medium collection

PC3 and DU145 cells were cultured in 10% FBS-DMEM medium. HUVECs were purchased from ScienCell Research Laboratories and grown in the ECM medium (ScienCell, Carlsbad, CA). Conditioned medium was collected from confluent PC3 cell cultures 24 hours after changing the medium to 0.2% FBS DMEM. The medium was filtered with 0.22 μm filters prior to being used.

Cell proliferation

PCa cells infected with shCtrl and shFrs2 lentivirus for 24 hours were seeded in 96-well plates at a density of 5,000 cells per well. After being cultured in 37°C for 48 hours, the cell densities were measured with the Cell Counting Kit-8 (Dojindo, Gaithersburg, MD). Data represent the mean ± sd of four wells.

Endothelial recruitment

PCa cells ($2.5x10^4$/well) seeded in 24-well plates were transfected with the indicated siRNAs. After being cultured in 37°C for 48 hours, the cells were washed with PBS and the culture media were replaced with 0.2% FBS EGM. Each well was then inserted a chamber with an 8.0 μm pore size membrane (BD Falcon) containing $1x10^5$ serum-starved HUVECs in 0.5 ml 0.2% FBS-ECM medium. After the co-culture for 32 hours at 37°C, HUVEC cells were fixed with 4% paraformaldehyde and stained with hematoxylin. Three randomly pick areas in each insert were imaged and numbers of migrated HUVEC cells in each imaged area were counted. Data are mean ± sd of 3 replicates.

Scratch wound healing

HUVECs ($1 x 10^5$ cells/well) were seeded in six-well plates pre-coated with 0.1% gelatin. The cells were grown to confluence, followed by serum-starvation overnight and mitomycin treatment to stop cell proliferation. A scratch in each well was made with a pipette tip. The cells were then cultured in the EGM containing 0.5% FBS with or without supplemented with PC3-conditioned media. The number of HUVECs that migrated were counted using a phase contrast microscope.

HUVEC tube formation

HUVECs ($2x10^4$) were seeded in 24-well plates containing 0.5 ml solidified Matrigel (10 mg/ml) and cultured in the EGM medium with or without supplementation of PC3 conditioned medium for 8–12 hours at 37°C. Images were acquired with a phase-contrast microscope. Average numbers of tubes were counted in three individual wells and presented as mean ± sd.

Gene silencing with siRNA or shRNA

siRNA targeting Frs2α, Hif1a, Ap2 and Sp1 were purchased from Dharmacon, GE health (Lafayette, CO, Catalog number: L-006440-00-0005, J-026959-08-0002, J-006348-06-0002 and J-004018-08-0002. PC3 cells were transfected with siRNA 48 hours before being used for functional assays. The coding sequences for shRNAs were cloned into the pLL3.7 plasmid for integrated into lentivirus. GIPZ lentiviral shRNA targeting *Frs2α* was obtained from Dharmacon, GE health (Lafayette, CO, Clone ID: V2LMM_90453). Stable cell lines containing Frs2 or non-silencing shRNAs were acquired by G418 selection.

Gene expression

Total RNA was extracted with the Ribopure RNA isolation reagent (Ambion, TX). Reverse transcription was carried out with SuperScript III (Life Technologies, Grand Island, NY) and random primers. Real-time PCR was performed on MX3000 (Strategene), using the SYBR

Green JumpStart Taq ReadyMix (Sigma, St. Louis, MO) with the primers list in Table 1 and following the manufacturer's protocol. The ratio between expression levels in the two samples was calculated by relative quantification, using β-actin as a reference transcript for normalization.

Western blot

Tumors or cultured cells were dissociated in 1% Triton X-100/PBS containing Proteinase and Phosphatase Inhibitors. The lysates were separated on SDS-PAGE and blotted onto PVDF membranes. The membranes were treated with 5% non-fat milk and incubated with primary antibodies overnight. Mouse anti-β-actin (1:2000) and rabbit anti cJUN (1:10000) antibodies were from Cell Signaling Technology; rabbit anti-VEGF (1:200) and mouse anti-VEGF antibodies from Abcam; rabbit anti-HIF1α (1:1000) from Novus Biologicals. After being washed with the TBST buffer, the membranes were incubated with horseradish peroxidase conjugated rabbit antibodies at room temperature for 1 hour. The specifically bound antibodies were visualized by using the ECL-Plus chemoluminescent reagents. For quantitative analysis, the films were scanned with a densitometer.

Chromatin immunoprecipitation (ChIP)

Cells transfected with control or shFrs2 lentivirus for 72 hours were lysed and subjected to ChIP analyses with the EZ-ChIP Kit from Millipore (Billerica, MA) according to the manufacturer's protocols. Rabbit anti-cJUN antibodies) and control IgG were purchased from Cell Signaling Technology (Beverly, MA). Mouse anti-HIF1α antibody was obtained from Novus Biologicals (Littleton, CO). The real-time PCR primers for the AP1-binding site regions were: Vegf-AP1 Forward (TAAGGGCCTTAGGACACCAT) and Vegf-AP1 Reverse (GGAATGCAGCAATTTCCCTC), and HIF1α-binding regions were: Vegf-HRE Forward (CAGGAACAAGGGCCTCTGTCT) and (TGTCCCTCTGACAATGTGCCATC).

Statistical analysis

Statistical analysis was performed by the two tailed t test, significance set to $P < 0.05$. Correlation between Frs2α and CD31 was determined by Pearson's correlation test. Survival analysis was examined using the Prism 6 software. Error bars indicate standard deviation.

Supplementary Material

Refer to Web version on PubMed Central for supplementary material.

Acknowledgments

We thank Dr. Stefan Siwko and Samantha Del Castillo for critical reading of the manuscript. This work was supported in part by the National Institutes of Health CA96824 and DE023106 to FW, CA140388 to NN, WLM and FW, and The Cancer Prevention and Research Institution of Texas CPRIT110555 to FW and WLM, and the National Natural Science Foundation of China 81170699, 81272813 to CW, 81101712, 81270761 to XL, 510180 to WZ, and 81072016 to ZYZ.

References

1. Acevedo VD, Gangula RD, Freeman KW, Li R, Zhang Y, Wang F, et al. Inducible FGFR-1 activation leads to irreversible prostate adenocarcinoma and an epithelial-to-mesenchymal transition. Cancer Cell. 2007; 12:559–571. [PubMed: 18068632]
2. Bergers G, Benjamin LE. Angiogenesis: Tumorigenesis and the angiogenic switch. Nature Reviews Cancer. 2003; 3:401–410. [PubMed: 12778130]
3. Cross MJ, Claesson-Welsh L. FGF and VEGF function in angiogenesis: signalling pathways, biological responses and therapeutic inhibition. Trends Pharmacol Sci. 2001; 22:201–207. [PubMed: 11282421]
4. Devilard E, Bladou F, Ramuz O, Karsenty G, Dales JP, Gravis G, et al. FGFR1 and WT1 are markers of human prostate cancer progression. BMC cancer. 2006; 6:272. [PubMed: 17137506]
5. Francescone RA 3rd, Faibish M, Shao R. A Matrigel-based tube formation assay to assess the vasculogenic activity of tumor cells. J Vis Exp. 2011
6. Giri D, Ropiquet F, Ittmann M. FGF9 is an autocrine and paracrine prostatic growth factor expressed by prostatic stromal cells. Journal of cellular physiology. 1999; 180:53–60. [PubMed: 10362017]
7. Giri D, Ropiquet F, Ittmann M. Alterations in expression of basic fibroblast growth factor (FGF) 2 and its receptor FGFR-1 in human prostate cancer. Clinical cancer research: an official journal of the American Association for Cancer Research. 1999; 5:1063–1071. [PubMed: 10353739]
8. Gotoh N, Ito M, Yamamoto S, Yoshino I, Song N, Wang Y, et al. Tyrosine phosphorylation sites on FRS2alpha responsible for Shp2 recruitment are critical for induction of lens and retina. Proceedings of the National Academy of Sciences of the United States of America. 2004; 101:17144–17149. [PubMed: 15569927]
9. Greenberg NM, DeMayo F, Finegold MJ, Medina D, Tilley WD, Aspinall JO, et al. Prostate cancer in a transgenic mouse. Proceedings of the National Academy of Sciences of the United States of America. 1995; 92:3439–3443. [PubMed: 7724580]
10. Hadari YR, Gotoh N, Kouhara H, Lax I, Schlessinger J. Critical role for the docking-protein FRS2 alpha in FGF receptor-mediated signal transduction pathways. Proceedings of the National Academy of Sciences of the United States of America. 2001; 98:8578–8583. [PubMed: 11447289]
11. Harris AL, Zhang H, Moghaddam A, Fox S, Scott P, Pattison A, et al. Breast cancer angiogenesis--new approaches to therapy via antiangiogenesis, hypoxic activated drugs, and vascular targeting. Breast Cancer Res Treat. 1996; 38:97–108. [PubMed: 8825127]
12. Huang X, Yu C, Jin C, Kobayashi M, Bowles CA, Wang F, et al. Ectopic activity of fibroblast growth factor receptor 1 in hepatocytes accelerates hepatocarcinogenesis by driving proliferation and vascular endothelial growth factor-induced angiogenesis. Cancer research. 2006; 66:1481–1490. [PubMed: 16452204]
13. Huang YQ, Han ZD, Liang YX, Lin ZY, Ling XH, Fu X, et al. Decreased expression of myosin light chain MYL9 in stroma predicts malignant progression and poor biochemical recurrence-free survival in prostate cancer. Medical oncology. 2014; 31:820. [PubMed: 24338276]
14. Jin C, McKeehan K, Guo W, Jauma S, Ittmann MM, Foster B, et al. Cooperation between ectopic FGFR1 and depression of FGFR2 in induction of prostatic intraepithelial neoplasia in the mouse prostate. Cancer research. 2003; 63:8784–8790. [PubMed: 14695195]
15. Jin C, McKeehan K, Wang F. Transgenic mouse with high Cre recombinase activity in all prostate lobes, seminal vesicle, and ductus deferens. The Prostate. 2003; 57:160–164. [PubMed: 12949940]
16. Li ZG, Mathew P, Yang J, Starbuck MW, Zurita AJ, Liu J, et al. Androgen receptor-negative human prostate cancer cells induce osteogenesis in mice through FGF9-mediated mechanisms. The Journal of clinical investigation. 2008; 118:2697–2710. [PubMed: 18618013]
17. Lin Y, Zhang J, Zhang Y, Wang F. Generation of an Frs2alpha conditional null allele. Genesis. 2007; 45:554–559. [PubMed: 17868091]
18. McDougall SR, Anderson AR, Chaplain MA. Mathematical modelling of dynamic adaptive tumour-induced angiogenesis: clinical implications and therapeutic targeting strategies. Journal of theoretical biology. 2006; 241:564–589. [PubMed: 16487543]
19. McKeehan, WL.; Wang, F.; Luo, Y. Handbook of Cell Signaling. 2. Vol. I. Academic/Elsevier Press; New York: 2009. The fibroblast growth factor (FGF) signaling complex.

20. Memarzadeh S, Xin L, Mulholland DJ, Mansukhani A, Wu H, Teitell MA, et al. Enhanced paracrine FGF10 expression promotes formation of multifocal prostate adenocarcinoma and an increase in epithelial androgen receptor. Cancer Cell. 2007; 12:572–585. [PubMed: 18068633]
21. Ozen M, Giri D, Ropiquet F, Mansukhani A, Ittmann M. Role of fibroblast growth factor receptor signaling in prostate cancer cell survival. Journal of the National Cancer Institute. 2001; 93:1783–1790. [PubMed: 11734594]
22. Pages G, Pouyssegur J. Transcriptional regulation of the Vascular Endothelial Growth Factor gene--a concert of activating factors. Cardiovascular research. 2005; 65:564–573. [PubMed: 15664382]
23. Polnaszek N, Kwabi-Addo B, Peterson LE, Ozen M, Greenberg NM, Ortega S, et al. Fibroblast growth factor 2 promotes tumor progression in an autochthonous mouse model of prostate cancer. Cancer research. 2003; 63:5754–5760. [PubMed: 14522896]
24. Song Z, Powell WC, Kasahara N, van Bokhoven A, Miller GJ, Roy-Burman P. The effect of fibroblast growth factor 8, isoform b, on the biology of prostate carcinoma cells and their interaction with stromal cells. Cancer research. 2000; 60:6730–6736. [PubMed: 11118059]
25. Taylor BS, Schultz N, Hieronymus H, Gopalan A, Xiao Y, Carver BS, et al. Integrative genomic profiling of human prostate cancer. Cancer Cell. 2010; 18:11–22. [PubMed: 20579941]
26. Teishima J, Yano S, Shoji K, Hayashi T, Goto K, Kitano H, et al. Accumulation of FGF9 in prostate cancer correlates with epithelial-to-mesenchymal transition and induction of VEGF-A expression. Anticancer research. 2014; 34:695–700. [PubMed: 24511001]
27. Tischer E, Mitchell R, Hartman T, Silva M, Gospodarowicz D, Fiddes JC, et al. The human gene for vascular endothelial growth factor. Multiple protein forms are encoded through alternative exon splicing. The Journal of biological chemistry. 1991; 266:11947–11954. [PubMed: 1711045]
28. Tsujii M, Kawano S, Tsuji S, Sawaoka H, Hori M, DuBois RN. Cyclooxygenase regulates angiogenesis induced by colon cancer cells. Cell. 1998; 93:705–716. [PubMed: 9630216]
29. Valencia T, Joseph A, Kachroo N, Darby S, Meakin S, Gnanapragasam VJ. Role and expression of FRS2 and FRS3 in prostate cancer. BMC cancer. 2011; 11:484. [PubMed: 22078327]
30. Valta MP, Tuomela J, Bjartell A, Valve E, Vaananen HK, Harkonen P. FGF-8 is involved in bone metastasis of prostate cancer. Int J Cancer. 2008; 123:22–31. [PubMed: 18386787]
31. Wan X, Corn PG, Yang J, Palanisamy N, Starbuck MW, Efstathiou E, et al. Prostate cancer cell-stromal cell crosstalk via FGFR1 mediates antitumor activity of dovitinib in bone metastases. Science translational medicine. 2014; 6:252ra122.
32. Wang F, McKeehan K, Yu C, Ittmann M, McKeehan WL. Chronic activity of ectopic type 1 fibroblast growth factor receptor tyrosine kinase in prostate epithelium results in hyperplasia accompanied by intraepithelial neoplasia. The Prostate. 2004; 58:1–12. [PubMed: 14673947]
33. Wang J, Stockton DW, Ittmann M. The fibroblast growth factor receptor-4 Arg388 allele is associated with prostate cancer initiation and progression. Clinical cancer research: an officialjournal of the American Association for Cancer Research. 2004; 10:6169–6178.
34. Wang X, Asmann YW, Erickson-Johnson MR, Oliveira JL, Zhang H, Moura RD, et al. High-resolution genomic mapping reveals consistent amplification of the fibroblast growth factor receptor substrate 2 gene in well-differentiated and dedifferentiated liposarcoma. Genes, chromosomes & cancer. 2011; 50:849–858. [PubMed: 21793095]
35. Weidner N, Carroll PR, Flax J, Blumenfeld W, Folkman J. Tumor angiogenesis correlates with metastasis in invasive prostate carcinoma. The American journal of pathology. 1993; 143:401–409. [PubMed: 7688183]
36. Winter SF, Acevedo VD, Gangula RD, Freeman KW, Spencer DM, Greenberg NM. Conditional activation of FGFR1 in the prostate epithelium induces angiogenesis with concomitant differential regulation of Ang-1 and Ang-2. Oncogene. 2007; 26:4897–4907. [PubMed: 17297442]
37. Yang F, Zhang Y, Ressler SJ, Ittmann MM, Ayala GE, Dang TD, et al. FGFR1 is essential for prostate cancer progression and metastasis. Cancer research. 2013; 73:3716–3724. [PubMed: 23576558]
38. Yu EM, Jain M, Aragon-Ching JB. Angiogenesis inhibitors in prostate cancer therapy. Discovery medicine. 2010; 10:521–530. [PubMed: 21189223]

39. Zhang K, Chu K, Wu X, Gao H, Wang J, Yuan YC, et al. Amplification of FRS2 and activation of FGFR/FRS2 signaling pathway in high-grade liposarcoma. Cancer research. 2013; 73:1298–1307. [PubMed: 23393200]

40. Zhang Y, Zhang J, Lin Y, Lan Y, Lin C, Xuan JW, et al. Role of epithelial cell fibroblast growth factor receptor substrate 2{alpha} in prostate development, regeneration and tumorigenesis. Development. 2008; 135:775–784. [PubMed: 18184727]

41. Zhong WD, Liang YX, Lin SX, Li L, He HC, Bi XC, et al. Expression of CD147 is associated with prostate cancer progression. International journal of cancer Journal international du cancer. 2012; 130:300–308. [PubMed: 21328337]

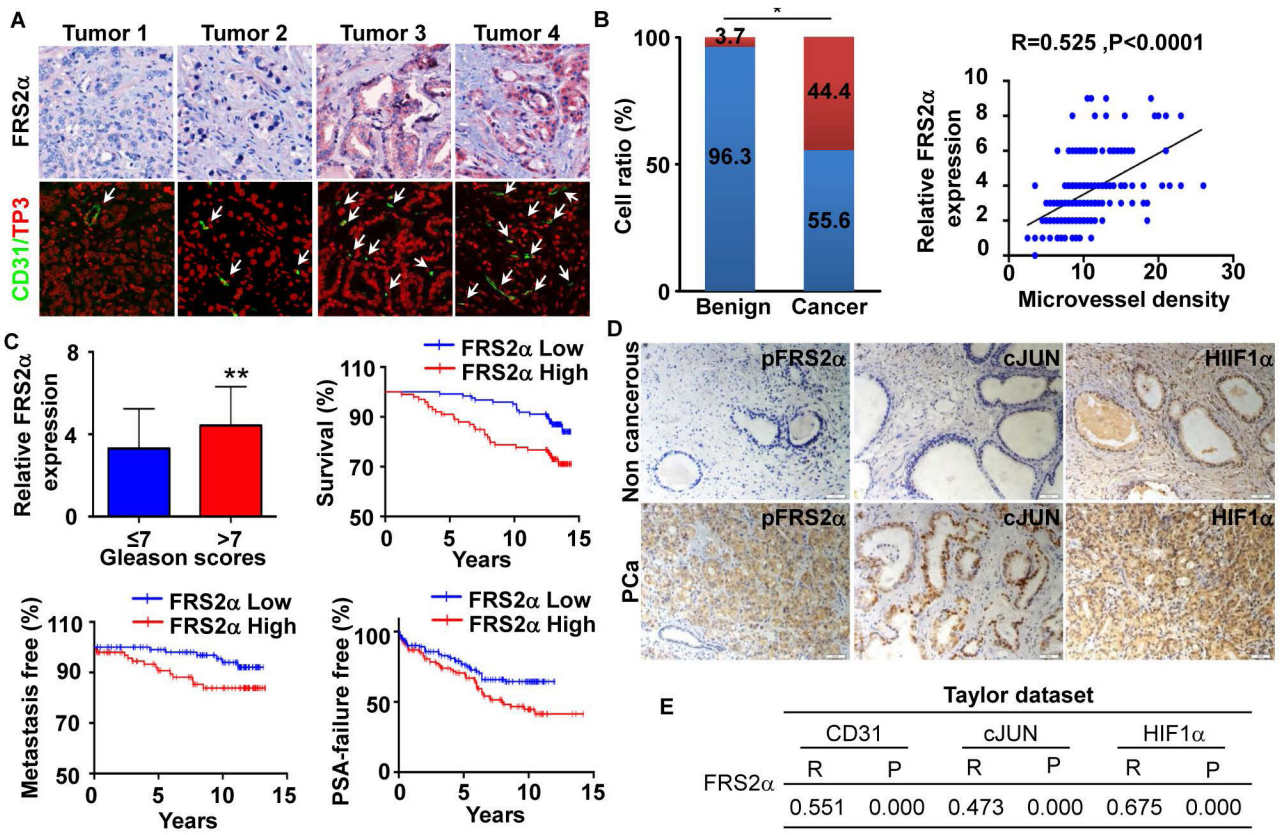

Fig. 1. Expression and activation of Frs2α in human PCa

A. Representative images of immunochemical staining of FRS2α and CD31 counterstained with nuclear To-Pro3 (TP3) in the MGH PCa TMA. **B.** Statistical comparison of differences in expression of FRS2α in human PCa and benign prostate (a) and Pearson correlation between FRS2α expression and microvessel density determined by CD31 staining (b). Red bar, FRS2α expression score>3; blue bar, FRS2α expression score≤3. **C.** Statistical analyses of the association of FRS2α expression with Gleason scores and survival time of the patients. **D.** Representative images of FRS2α phosphorylation and expression of the indicated molecules in PCa TMA (from Shanghai Outdo Biotech Co, LTD). **E.** Statistical analyses of the association between Frs2α and CD31, cJun, or Hif1a expression at the mRNA level in the Taylor dataset. R, Pearson correlation coefficient; P, *p* value; *, $P<0.05$

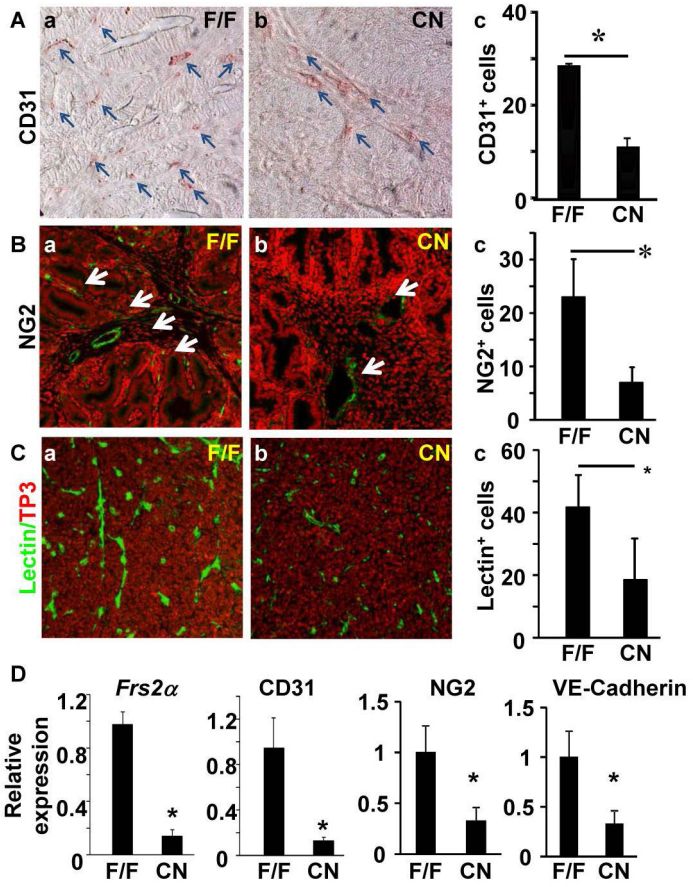

Fig. 2. Ablation of *Frs2α* in prostate epithelial cells reduces angiogenesis in mouse TRAMP tumors

A–C. Prostate tumor sections of 5-month-old TRAMP mice bearing floxed (F/F) (n=7) or epithelial-specific null (CN) (n=8) *Frs2α* alleles were stained with the indicated antibodies or lectins. The average number of stained cells per viewing frame was scored as indicated in panel c. **D.** Real-time RT-PCR analyses of the indicated mRNA in TRAMP tumors with or without *Frs2α* ablation. Data were normalized with β-actin and were expressed as mean ± sd from triplicate samples. TP3, To-Pro3; *, $P<0.05$.

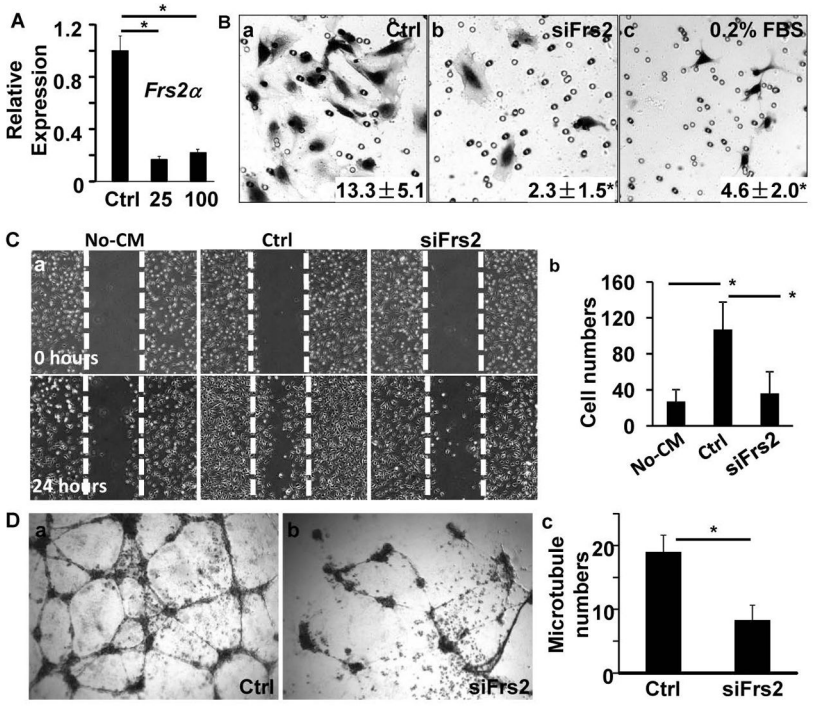

Fig. 3. Depletion of FRS2α in PC3 cells reduces ability to induce HUVEC migration

A. Real-time RT-PCR analyses of FRS2α expression in PC3 cells treated with control or FRS2α siRNA at the indicated concentration. **B.** Transwell assays with HUVECs in the upper chamber and 10% PC3 cell-conditioned medium or 0.2% FBS in the lower chamber. Number of cells that migrated through the membrane was counted from triplicate samples and shown as means ± sd. **C.** Confluent HUVEC cultures were injured by linear scrape with a pipette tip followed by addition of medium containing indicated PC3 cell conditioned medium for 24 hours. Panel a, images before and after culture for 24 with the indicated conditioned medium. Panel b, average number of cells that migrated from 3 independent samples. **D.** HUVECs were inoculated in Matrigel with 10% of medium conditioned by PC3 cells treated with control or FRS2α siRNA. The indicated images of HUVECs were captured after cultured in 37°C for 8 hours. The average number of tubes formed from HUVECs were calculated from triplicate samples and presented as mean ± sd (c). Ctrl, control siRNA; 25 and 100, 25 μM and 100 μM FRS2α siRNA, respectively; no-CM, negative control without conditioned medium; *, $P<0.05$.

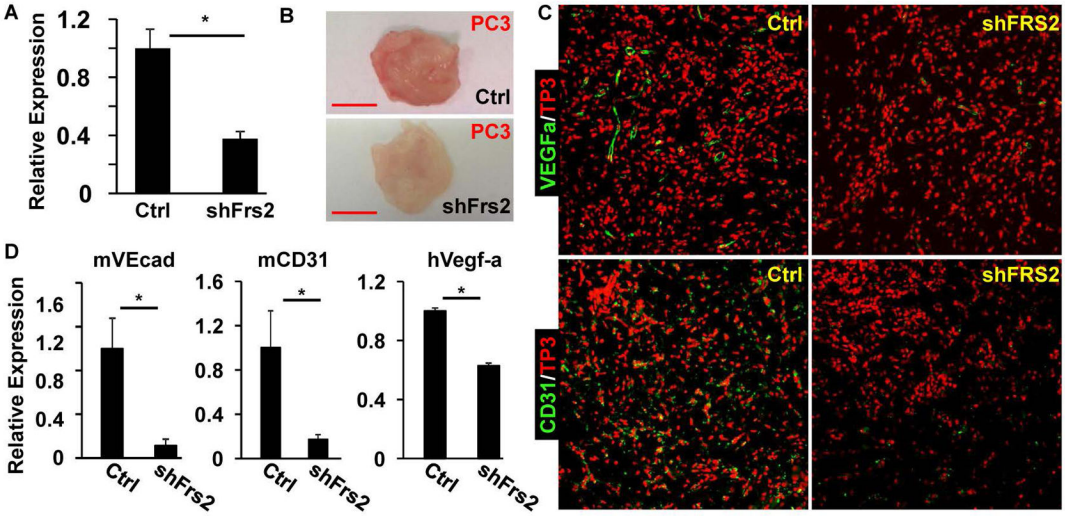

Fig. 4. Depletion of FRS2α in PC3 cells in Matrigel plugs dampens recruitment of endothelial cells into the plugs in nude mice

A. Real-time RT-PCR analyses of Frs2α expression in PC3 cells infected with lentivirus carrying FRS2α or control shRNA. **B.** Gross morphology of the Matrigel plugs harvested from nude mice at two weeks after the implantation. **C**. Immunostaining of Matrigel plug sections with anti-CD31 or anti-VEGF-A antibodies. To-Pro3 (TP3) was used for nuclear counter staining. **D**. Real-time RT-PCR analyses of the RNA extracted from the Matrigel plugs containing control (n=6) or FRS2α-depleted (n=6) PC3 cells. mVEcad, mouse VE-cadherin; mCD31, mouse CD31; hVegf-a, human Vegf-a; shFRS2, FRS2α shRNA; Ctrl, control shRNA; *, $P<0.05$.

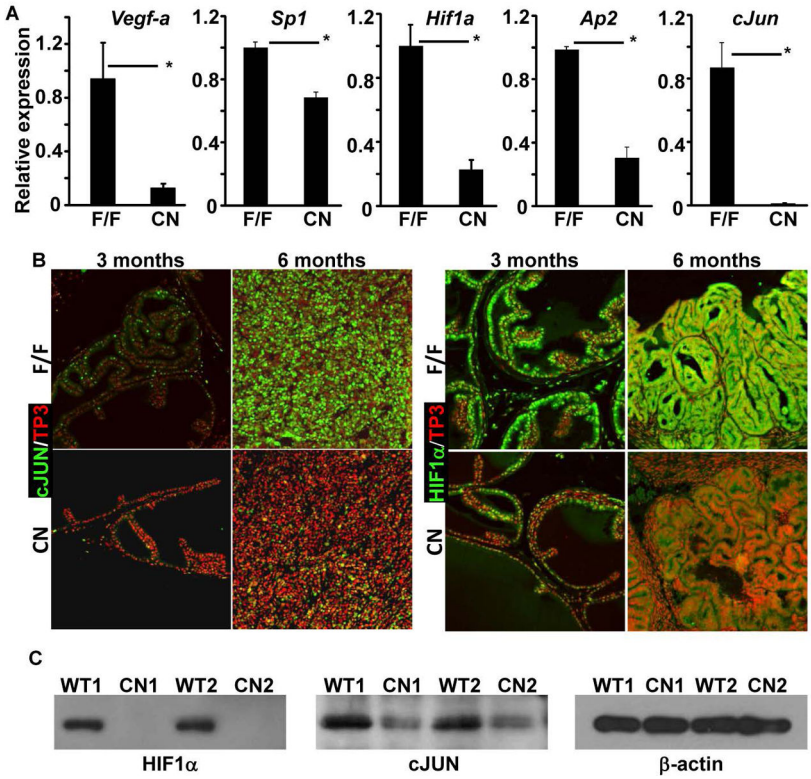

Fig. 5. Depletion of FRS2*α* reduces expression of *Vegf-a* in mouse TRAMP tumors

A. Real-time RT-PCR analyses of the indicated gene expression in TRAMP tumors with or without tissue-specific ablation of *Frs2α* in the epithelial cells. **B&C**. Immunostaining (B) and Western blot (C) analyses of cJUN and HIF1α expression in the TRAMP tumors. F/F, $Frs2\alpha^{flox}$; CN, $Frs2\alpha^{CN}$; *, $P<0.05$.

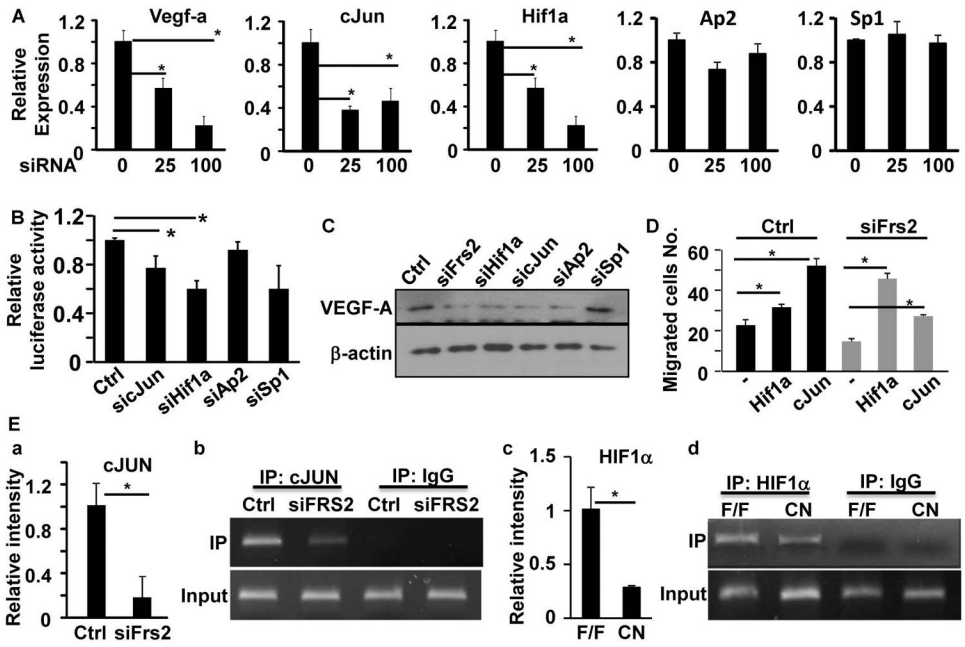

Fig. 6. Depletion of *Frs2α* in PCa cells reduces expression of *Vegf-a*

A. Real-time RT-PCR analyses of PC3 cells at 72 hours after treatment with the indicated siRNA at a final concentration of 25 or 100 mM. **B**. Luciferase reporter analyses of Vegf-a reporter activities in PC3 cells with or without depletion of expression of the indicated genes. **C**. Western blot analyses of VEGF-A expression in PC3 cells after reduction in expression of the indicated genes. **D.** Transwell cell culture analyses of HUVECs treated with conditioned medium of PC3 cells overexpressing cJUN or HIF1α. **E**. ChIP assays of Vegf-a promoter with anti-cJUN or anti-HIF1α antibodies. Panels a and c are the relative binding of cJUN or HIF1α to the V egf-A promoter. Data are mean ± sd derived from 3 replicate samples. Panels b and d are images of agarose gel electrophoresis showing single band of the PCR products. Ctrl, control siRNA; IP, immunoprecipitation; F/F, $Frs2\alpha^{flox}$; CN, $Frs2\alpha^{CN}$; *, $P<0.05$.

Table 1

Primers for real time RT-PCR analyses

Gene Name		Sequence (from 5′-3′)
Human Vegf-a	forward	CGAACGTACTTGCAGATGTG
	reverse	CTGTTCTGTCGATGGTGATG
Human Hif1α	forward	TCCAAGAAGCCCTAACGTGT
	reverse	TGATCGTCTGGCTGCTGTAA
Human cJun	forward	TTTCAGGAGGCTGGAGGAAG
	reverse	CTGCCACCAATTCCTGCTTT
Human sp1	forward	TTGAAA AAGGAGTTGGTGGC
	reverse	TGCTGGTTCTGTAAGTTGGG
Human Frs2α	forward	TCCAGGATTTGCTGCTCAGA
	reverse	TTTCCGCTCTTCTTGCACAC
Human Ap2	forward	TGGATCCTCGCAGGGAC ACAG
	reverse	GTTGGACTTGGACAGGGACAC G
Human GAPDH	forward	GAAGGTCGGAGTCAACGGATT
	reverse	TGACGGTGCCATGGAATTTG
Mouse *Vegf-a*	forward	ACCTCCACCATGCCAAGT
	reverse	TCAATCGGACGGCAGTAG
mouse *Hif1α*	forward	GTGAACAGAATGGAACGGAG
	reverse	CACAATCGTAACTGGTCAGC
Mouse *c-Jun*	forward	CATAGCCAGAACACGCTTCC
	reverse	TTGAAGTTGCTGAGGTTGGC
Mouse *Sp1*	forward	TGGTCATATTGTGGGAAGCG
	reverse	AATAAGGGCTGAAGGAGTGG
Mouse *Frs2α*	forward	GAGCTGGAAGTCCCTAGGACACCT
	reverse	GCTCTCAGCATTAGAAACCCTTGC
Mouse *Ap2*	forward	GATGAAATCACCGCAGACGA
	reverse	TCCTTTGGCTCATGCCCTTT
Mouse *VE-cadherin*	forward	TTGGGCTTTCTGACTGTTGT
	reverse	CAGGGACTTCGTGGGTTT
Mouse *β-actin*	forward	GCACCAAGGTGTGATGGTG
	reverse	GGATGCCACAGGATTCCATA